Cancer Cell International

RESEARCH Open Access

The sEVs miR-487a/Notch2/GATA3 axis promotes osteosarcoma lung metastasis by inducing macrophage polarization toward the M2-subtype

Piaopiao Wang[1], Lei Yang[2], Jing Dong[1], Wenjing Liu[1], Fan Xie[1], Yan Lu[1] and Wenyan Li[1*]

Abstract

Small extracellular vesicles (sEVs) are important mediators of intercellular communication between tumor cells and their surrounding environment. Furthermore, the mechanisms by which miRNAs carried in tumor sEVs regulate macrophage polarization remain largely unknown. To concentrate sEVs, we used the traditional ultracentrifugation method. Western blot, NanoSight, and transmission electron microscopy were used to identify sEVs. To determine the function of sEVs-miR-487a, we conducted in vivo and in vitro investigations. The intercellular communication mechanism between osteosarcoma cells and M2 macrophages, mediated by sEVs carrying miR-487a, was validated using luciferase reporter assays, transwell assays, and Western blot analysis. In vitro, sEVs enriched in miR-487a and delivered miR-487a to macrophages, promoting macrophage polarization toward an M2-like type, which promotes proliferation, migration, invasion, and epithelial-mesenchymal transition (EMT) of osteosarcoma cells. In vivo, sEVs enriched in miR-487a facilitate lung metastasis of osteosarcoma. Moreover, plasma miR-487a in sEVs was shown to be a potential biomarker applicable for osteosarcoma diagnosis. In summary, miR-487a derived from osteosarcoma cells can be transferred to macrophages *via* sEVs, then promote macrophage polarization towards an M2-like type by targeting Notch2 and activating the GATA3 pathway. In a feedback loop, the activation of macrophages accelerates epithelial-mesenchymal transition (EMT), which in turn promotes the migration, invasion, and lung metastasis of osteosarcoma cells. This reciprocal interaction between activated macrophages and osteosarcoma cells contributes to the progression of the disease. Our data demonstrate a new mechanism that osteosarcoma tumor cells derived exosomal-miR-487a which is involved in osteosarcoma development by regulating macrophage polarization in tumor microenvironment (TME).

Keywords Small extracellular vesicles, M2 macrophages polarization, Notch2/GATA3, Osteosarcoma lung metastasis

*Correspondence:
Wenyan Li
liwenyan_linda@163.com
[1]Department of Clinical Pharmacy, Gongli Hospital of Shanghai Pudong New Area, 219, Miaopu Road, Pudong New Area, 200135 Shanghai, China
[2]Department of Orthopedics, Taizhou School of Clinical Medicine, Taizhou People's Hospital of Nanjing Medical University, Nanjing Medical University, 225300 Taizhou, Jiangsu, China

Introduction

Primary osteosarcoma (OS) is one of the most prevalent bone tumors, with a particularly high incidence in children and adolescents [1]. Additionally, the propensity of osteosarcoma to undergo early-stage distant metastasis contributes to a poor prognosis for patients [2]. Epithelial mesenchymal transition (EMT) plays a crucial role in the process of tumor metastasis, which is associated with the communication between cancer cells and tumor microenvironment (TME) [3]. The tumor microenvironment (TME) is composed of a complex network that includes tumor-infiltrating immune cells, mesenchymal stem cells, cancer cells, and inflammatory mediators [4]. Tumor-associated macrophages (TAMs) are the predominant immune cells that infiltrate the tumor microenvironment [5]. They are essential phagocytes of the innate immune system and have been associated with the survival of patients with osteosarcoma [6]. Previous research has shown that inhibiting TAMs polarization prevents the formation of human osteosarcoma [7]. Specifically, under the influence of the local microenvironment, TAMs can differentiate into two distinct subsets: a tumor-destructive M1 phenotype and an M2-like protumoral phenotype [8]. M1 macrophages play a role in damaging tumor cells by producing pro-inflammatory chemical substances and cytokines, such as IL-12, iNOS, and TNF-α. They also support adaptive immune responses [9]. On the contrary, M2 macrophages play a detrimental role, promoting tumor metastasis and resulting in poor patient survival [10].

Previous studies have showed that the Notch pathway plays an important role in EMT during tumor metastasis [11]. Notch 2 is a receptor belonging to the Notch family. It can be activated when it binds to its ligands, leading to the cleavage and release of the Notch2 intracellular domain (N2ICD) [12]. The N2ICD can translocate to the nucleus, where it interacts with the transcription factor RBPJ. This interaction triggers a series of activations of target genes that are involved in EMT [13]. Furthermore, the activation of the Notch pathway is necessary for GATA3-induced IL-4 secretion [14–16]. IL-4, in turn, can induce the polarization of macrophages towards the M2 phenotype. Additionally, the activated Notch pathway is associated with EMT and regulates the polarization of macrophages within the tumor microenvironment [17]. Accumulating studies support the functional crosstalk between the Notch pathway and EMT.

SEVs, cell-secreted < 200 nm vesicles, derived by virtually all cell types and identified in various body fluids [18]. These sEVs contain various functional molecules and play a vital role in communication, signal transduction, diagnosis, regulation of immune response, and drug delivery [19, 20]. SEVs were derived from tumor cells that could taken up by macrophages, and then regulated macrophage polarization. MicroRNAs (miRNAs) are indeed the cargoes carried by SEVs, and they can bind to the 3'UTR of target mRNA. This binding enables them to regulate the development of multiple tumors. For instance, colorectal cancer cell-derived sEVs-miR-934 facilitates metastasis of tumor *via* inducing the polarization of macrophages to M2 type [21]. Hypoxic pancreatic tumor cell-derived SEVs-miR-301a that promote macrophages toward to M2 phenotype. Numerous scholars have confirmed that miR-487a promotes the proliferation of cancer cells and is up-regulated in certain tumor tissues [20, 22, 23]. However, it remains unclear whether osteosarcoma cells derived from SEVs-miR-487a promote lung metastasis and EMT of osteosarcoma cells. Given that Notch2 was identified as a target of miR-487a, it was postulated that the miR-487a/Notch2/GATA3 axis regulates EMT and triggers IL-4 production in osteosarcoma cells. Furthermore, elevated IL-4 levels have been demonstrated to promote macrophage polarisation towards the M2 phenotype.

The current study has identified that osteosarcoma cells produce sEVs-miR-487a, which can enhance macrophage polarization towards M2-like polarization by targeting Notch2 via GTAT3-induced IL-4 release. This process has been shown to induce M2 macrophages, which in turn has increased osteosarcoma cell migration, invasion, EMT, and lung metastasis.

Materials and methods

Patients and tissue samples

The study collected osteosarcoma tissues and adjacent non-tumor tissues from patients at Taizhou People's Hospital of Nanjing Medical University. Both the non-tumor tissues and tumor tissues were histologically confirmed. Tissue samples were cryopreserved in liquid nitrogen for storage. Peripheral blood samples were collected from healthy human volunteers. All experiments involving humans and animals were approved by the Ethics Committee of Taizhou People's Hospital of Nanjing Medical University, Jiangsu, China.

The isolation of peripheral blood macrophages

The Ficoll density gradient (Catalog #60-00092-11, PluriSelect, Germany) was used to extract peripheral blood mononuclear cells (PBMC) from healthy male volunteer blood. Then, the monocytes were isolated with EasySep™ human monocyte isolation kit (Catalog #19059, Stemcell technologies, USA) as protocol. The adherent monocytes were cultured using RPMI-1640 which contained 10% FBS. The monocytes

differentiated into macrophages with the stimulation of 50 ng/mL macrophages colony-stimulating factor (M-CSF). Flow cytometry was used to determine the percentage of monocytes by CD14 staining (purity ≥ 95%), as previously described in the article [24].

Cell culture

Human osteosarcoma cell lines (143-B, HOS, Saos-2, MG63, and U2OS) were obtained from the National Collection of Authenticated Cell Cultures (Shanghai, China). The American Type Culture Collection (ATCC, Manassas, USA) provided normal human osteoblast hFOB 1.19 cells, which were grown in DMEM/F12 (Gibco, Carlsbad, USA) media. MEM (Gibco, Carlsbad, USA) served to cultivate MG63 and HOS cells, while McCoy's 5 A (Invitrogen, Carlsbad, CA, USA) was used to culture Saos-2, U2OS, and 143-B cells, all media contained 10% fetal bovine serum (FBS, Thermo, USA), 1% penicillin/streptomycin. MiR-487a mimics miR-487a inhibitor vectors, and si-Nothc2, which were obtained from GenePharma (Shanghai, China). Cell transfections were carried on as per the manufacturer's protocol.

Luciferase reporter assay

Macrophage cells (6×10^4) were collected and added to a 24-well plate. To create the luciferase construct, we co-transfected macrophages with Notch2-3'-UTR (wild-type or mutant) and miR-487a mimics or inhibitors with lipofectamine 2000 reagent (Invitrogen, Carlsbad, CA, USA). After 48 h, the cells were collected, and their luciferase activity was measured using a luciferase reporter gene assay kit (Promega, Madison, Wisconsin, USA).

Reverse transcription-quantitative polymerase chain reaction

The method used to detect miRNA expression followed the procedure previously reported in the article [25]. Total RNA was obtained using TRIzol (Thermo Fisher Scientific, San Jose, C, USA), and miRNA was extracted using the PureLinkTM miRNA Isolation Kit (Invitrogen, Carlsbad, CA, USA) as directed, and then identified using qRT-PCR. U6 and GAPDH served as the reference genes of miRNA and the other mRNA separately. The relative expression of genes was determined using $2^{-\Delta\Delta CT}$, and the primes are shown in Table S1.

Separation, concentration, and identification of sEVs

The FBS was ultracentrifuged at 120,000 g for 18 h to eliminate sEVs at 4 ℃. SEVs were isolated and characterized as our previously reported [26]. The supernatant from 48-hour cell cultures was centrifuged at 4 °C for 300 g (10 min), 2000 g (10 min), and 10,000 g (30 min) to isolate sEVs and remove debris and damaged cells. To obtain concentrated SEVs, the precipitates were resuspended in PBS after undergoing two rounds of ultracentrifugation at 120,000 g for two hours each. We used western blot analysis to evaluate the SEVs markers CD63, HSP70, and Alix. The morphology of sEVs was investigated using transmission electron microscopy (TEM, Hitachi, Tokyo, Japan). The diameter and particle concentration of sEVs were examined using the NanoSight NS300 microscope (Malvern, UK). We used concentrated SEVs in every experiment.

Transwell migration and invasion assays

Tumor cells (MG-63 and HOS) were implanted into a 12-well chamber (for migration) or a Matrigel chamber (for invasion) plate (5,000 cells/well) following the manufacturer's instructions (BD Bioscience, Bedford, MA, USA). Serum-free medium was used to dilute 4×10^4 cells, which were then seeded in the top chamber and the entire medium was poured into the lower chamber. The migration or invasion cells in the bottom compartment were stained with 0.1% crystal violet and preserved with methanol after 48 h.

Western blot assays

After collection, sEVs, cells, and tumor tissues were resuspended in lysis buffer (Sigma Aldrich, USA) and allowed to incubate for 30 min on ice. The supernatant was extracted for Western blotting following a 20-minute centrifugation at 12,000 g. The Western blot was performed as previously mentioned. Primary antibodies used in the experiment included anti-GAPDH (#ab77109), anti-CD14 (#ab282377), anti-CD163 (#ab112384), Notch2 (#ab114827), GATA3 (#ab199428) (1:1000, abcam, Cambridge, UK), anti-Alix (#92880), Calnexin (#2679), IL-4 (#12227) (1:1000, CST), anti-E-cadherin, anti-N-cadherin, anti-Vimentin (#AG3556), Twist (#AF8274), TSG101(#AF8259) (1:1000, Beyotime, Beijing, China).

Enzyme-linked immunosorbent assay (ELISA)

To investigate the impact of sEVs derived from MG-63 and HOS cells on macrophage expression of iNOS, CD86, and CD163.ELISA was performed using a human Arg-1 (#EK1316, Multi Sciences, Hangzhou, China), Ym1 (#DY2599, R&D system, USA), CD163 (#DC1630, R&D system), iNOS (#CB11694-Hu, Coibo Bio, Shanghai, China) and CD86 (#CB15455-Hu, Coibo Bio, Shanghai, China) ELISA kit as protocol. The absorbance of the samples was detected at 490 nm.

The cell counting kit-8 (CCK-8) assay

The cells were seeded into 96-well plates at a concentration of 5×10^4 cells/mL with 100 µL/well. They were then cultured at 37 °C with 5% CO2 for 24 h. Next, media, M-PBS, M-MG-63 sEVs, and M-HOS-63 sEVs were added to the respective wells with five replicate wells for each concentration. After 48 h of culture, cell viability was assessed using the CCK-8 kit according to the provided instructions.

Animal experiment

Using four-week-old male, specific pathogen-free BALB/c nude mice, we applied a lung metastasis paradigm to study the in vivo metastasis of sEVs generated from MG-63 cells 2×10^6 MG-63 cells mixed with pretreated macrophages (1:3) were transplanted into BALB/c mice via tail vein [27]. A total of 18 mice were randomly divided into three groups. All groups included MG-63 (control), MG-63 + macrophages pretreated with PBS (M-PBS), and MG-63 + macrophages pretreated with MG-Exos. After six weeks, the mice were sacrificed, and the lungs were removed for further investigation.

Statistical analysis

The mean ± standard deviations (SD) were displayed for all the data. MiR-487a expression and clinicopathological features in patients with osteosarcoma were compared using the Pearson χ^2test. The Student's *t*-test or one-way ANOVA was used to examine the differences between the groups. A statistically significant *P* value was defined as 0.05.

Results

MiR-487a is highly expressed in osteosarcoma

Initially, differential expression gene analyses were conducted on osteosarcoma patient tissues dataset GSE65071 and cell lines dataset GSE28423. The top 15 miRNAs from the GSE65071 dataset with the most significant fold change were further examined, as demonstrated by the heatmaps (Fig. 1A). For the cell lines dataset GSE28423, we also focused on the top 15 miRNAs with the largest fold changes (Fig. 1B). Subsequently, Venn diagram analysis revealed 13 genes at the intersection (Figure S1). In osteosarcoma tissues and various osteosarcoma cell lines, miR-487a was discovered to be an up-regulated miRNA (Fig. 1C and D). Thus, our research focused on miR-487a and explored

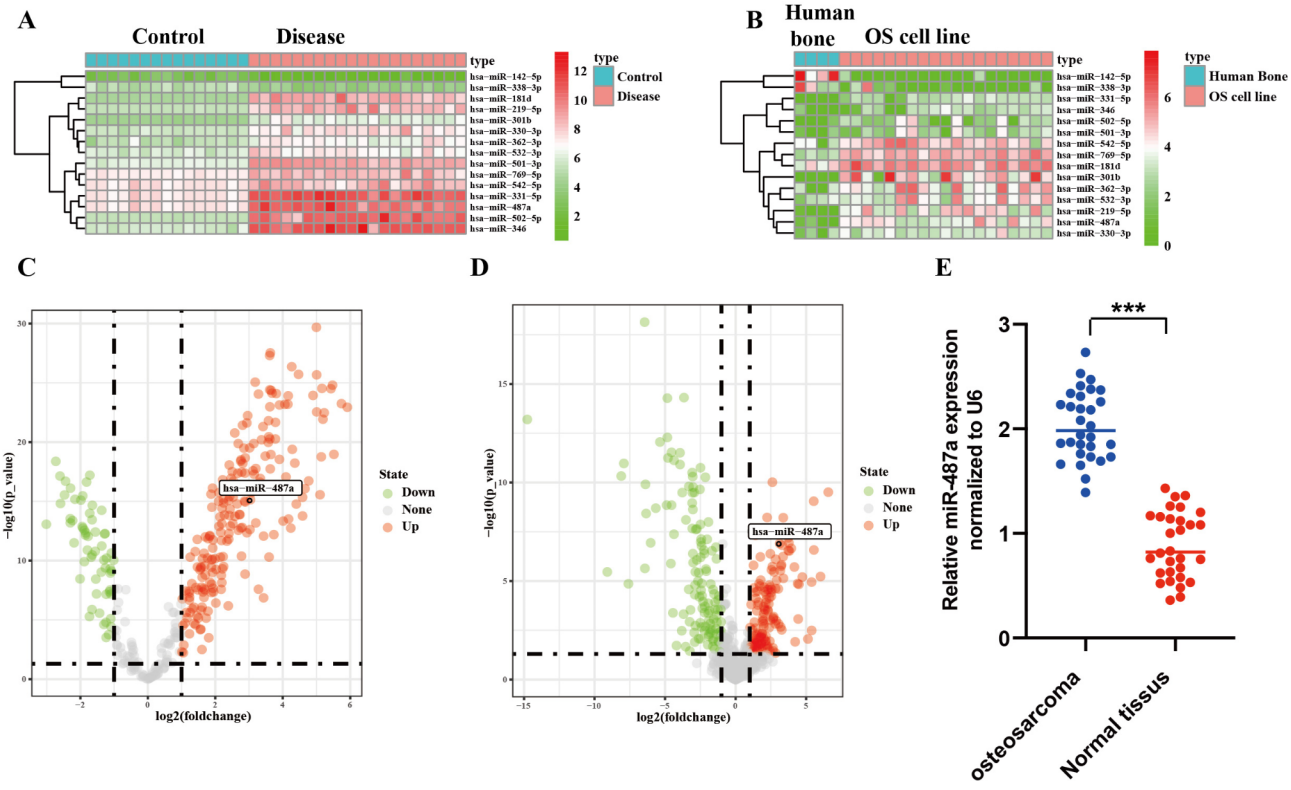

Fig. 1 The miR-487a is highly expressed in osteosarcoma. (**A**) The top 15 miRNAs with the largest fold change from the GSE65071 dataset were shown as heatmaps. (**B**) The top 15 miRNAs with largest fold change from the GSE28423 dataset were showed as heatmaps. (**C-D**) miR-487a was found to be an up-expressed miRNA in osteosarcoma tissues and various osteosarcoma cell lines. (**E**) The expression level of miR-487a in osteosarcoma tissues and adjacent tissues was detected using qRT-PCR (*p<0.05; **p<0.01; ***p<0.001)

its association with osteosarcoma. Furthermore, we found that osteosarcoma tissues expressed higher levels of miR-487a than adjacent tissues. (Fig. 1E).

MiR-487a is contained in the osteosarcoma cell-derived sEVs

We measured the levels of miR-487a in the medium of five osteosarcoma cell lines and one normal bone cell line, hFOB1.19, to investigate the significance of miR-487a in osteosarcoma patients. As shown in Fig. 2A, the expression level of miR-487a in the medium of MG-63 and HOS cells was significantly higher compared to the medium of other cell lines. MiR-487a was found to be most abundant in the medium, followed by the cytoplasm, and least abundant in the nucleus. Furthermore, the expression level of miR-487a in the medium of osteosarcoma cells remained unchanged after treatment with RNase A alone. However, when treated with a combination of RNase A and Triton X-100, the levels of miR-487a were significantly reduced (Fig. 2C). This suggests that miR-487a is encapsulated within the sEVs and not secreted directly into the medium.

Next, sEVs were isolated from MG-63 (MG-63 Exos) and HOS (HOS Exos) conditioned medium. To examine the morphology of sEVs, transmission electron microscopy (TEM) was employed. NTA was used to evaluate the concentration and size distribution of sEVs, and TEM indicated a spherical shape with a diameter between 30 and 150 nm (Fig. 2D and E). The markers of sEVs were identified using western blot analysis. The results showed the presence of CD63, TSG101, and Alix markers in the isolated sEVs (Fig. 2F). However, the endoplasmic reticulum marker calnexin was not detected in the isolated sEVs. These findings confirmed that the separated vesicles were sEVs. We used GW4869 to block the secretion of sEVs from osteosarcoma cells to determine if miR-487a was present. As seen by Fig. 2G, the miR-487a expression level in the GW4869 group was much lower than that in the sEVs group produced from osteosarcoma cells. Additionally, RT-qPCR was used to measure the expression level of miR-487a in sEVs from MG-63 and HOS. The expression pattern of miR-487a in sEVs validated the findings in Fig. 2B and C, as demonstrated in Fig. 2H. This suggested that the majority of the miR-487a was present in sEVs produced from MG-63 and HOS cells.

Osteosarcoma cell-derived sEVs-miR-487a promotes the polarization of macrophages towards M2 subtype

In this study, the GSE33382 dataset was preprocessed and osteosarcoma samples were retained for further analysis. Immune infiltration analysis showed that macrophages constituted the highest percentage of immune cells in osteosarcoma samples (Fig. 3A). Using TargetScan, we analyzed the 129 target genes of miR-487a and found that 53 of these genes were positively associated with M2 macrophages (Fig. 3B). Therefore, we hypothesize that miR-487a contained in the sEVs can facilitate tumor development by modulating the polarization of macrophages. As CD14 is the PBMC monocyte marker, the expression level of CD14 was determined with flow cytometry and our data suggested that most of the isolated cells were positively expressed CD14 (Fig. 3C, $^{**}p<0.01$). The miR-487a mimics were transfected into macrophages to observe the impact of miR-487a on their polarization. As shown in Fig. 3D, the M2 markers (Arg-1, Ym1, and CD163) were remarkably elevated after treatment with miR-487a mimics, whereas the M1 markers (iNOS and CD86) remained unchanged. To investigate the impact of exosomal-miR-487a produced by OS cells on macrophage polarization, we co-cultured macrophages with MG-63 and HOS sEVs. The expression levels of M2 markers CD163, were significantly increased after treatment with MG-63 sEVs and HOS sEVs (Fig. 3E). The RT-qPCR and ELISA expression levels of M2 markers, including Arg-1, Ym1, and CD163, were significantly increased after treatment with MG-63 sEVs and HOS sEVs (Fig. 3F and G). These findings suggest that the expression levels of M2 markers, including Arg-1, Ym1, and CD163, were elevated compared to the control group. Furthermore, in a more significant observation, we silenced miR-487a in osteosarcoma cells and subsequently isolated sEVs (MG-63 siR-487a Exos and HOS siR-487a Exos) for co-culture experiments with macrophages. We found that the sEVs with silenced miR-487a lose the ability to polarize macrophages towards the M2-subtype (Fig. 3H and I). All the findings indicate that the levels of M2 makers were strikingly raised in macrophages after treatment with osteosarcoma cells derived from sEVs-miR-487a.

sEVs-miR-487a target Notch2 and induce M2 polarization by activating GATA3

We explored the underlying mechanisms of sEVs-miR-487a that can polarize macrophages to M2 type. Based on the prediction from the TargetScan website, miR-487a has a specific binding region in Notch2 in its 3'-UTR (Fig. 4A). To confirm whether miR-487a targets Notch2, we transfected macrophages with miR-487a mimics or inhibitors and their respective empty vectors. To assess the effects, qRT-PCR and western blot analysis were conducted to measure the mRNA and protein expression levels of Notch2 (Fig. 4B and C). There is a possibility that miR-487a binds to the 3'-UTR of Notch2 to regulate its function. The result

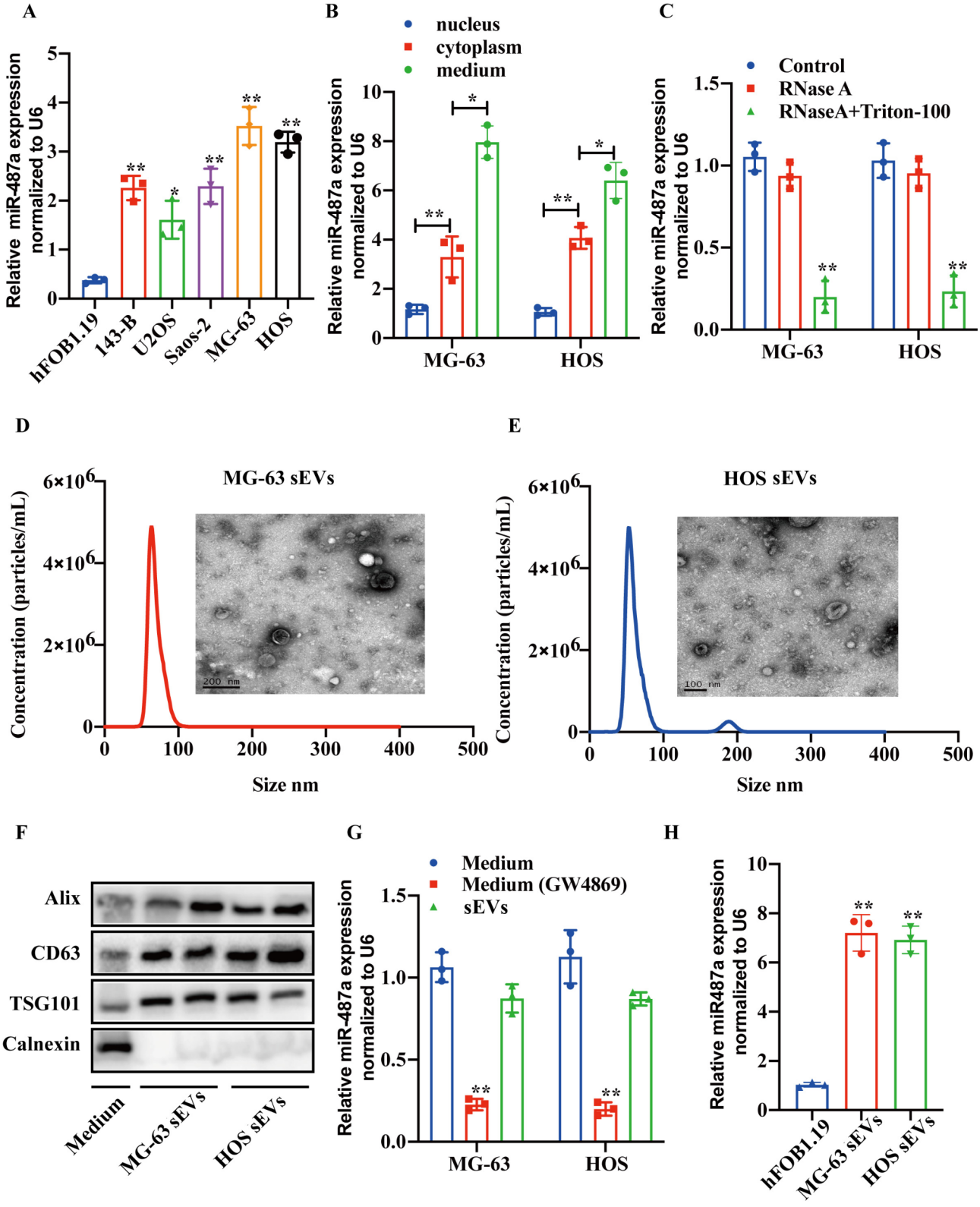

Fig. 2 miR-487a is contained in the osteosarcoma cell-derived sEVs. (**A**) qRT-PCR was used to identify the expression of miR-487a in various osteosarcoma cell media. (**B**) qRT-PCR was used to assess the expression of miR-487a in the cytoplasm, nucleus, and medium of MG-63 and HOS cells. (**C**) After co-culturing MG-63 and HOS cells with normal media, RNase A, or RNase A with Triton X-100, the expression of miR-487a was found. (**D**, **E**) TEM and NTA were used to determine the morphology, concentration, and size distribution of sEVs. (**F**) Western blotting revealed the presence of the sEVs Alix, CD63, and TSG101 markers. (**G**) qRT-PCR was used to determine the expression of miR-487a in condition media, which is normal medium supplemented with sEVs inhibitor (GW4869). (**H**) qRT-PCR was used to identify the expression of miR-487a in hFOB1.19 cells, MG-63 sEVs, and HOS sEVs. (*p<0.05; **p<0.01; ***p<0.001)

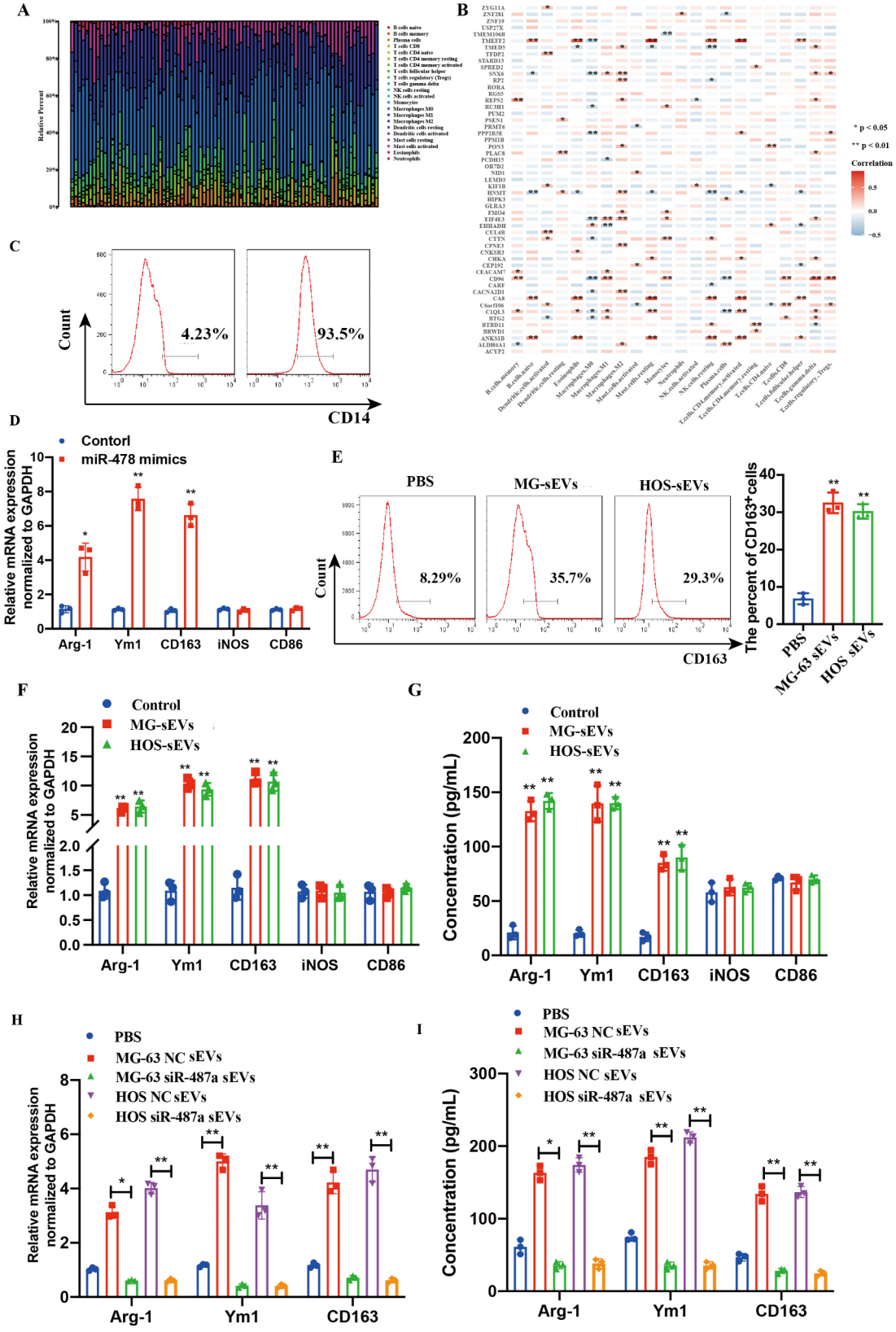

Fig. 3 (See legend on next page.)

(See figure on previous page.)

Fig. 3 Osteosarcoma cell-derived exosomal-miR-487a promotes macrophages polarization toward to M2-like phenotype. (**A**) After preprocessingGSE33382, only samples of osteosarcoma were retained. Analysis of osteosarcoma tissues using CIBERSORT, followed by determination of the percentage of macrophages in tumor tissues. (**B**) Correlation between miR-487a expression and distinct gene signatures of various immune cells. (**C**) FCM was used to identify the macrophage marker CD14. (**D**) qRT-PCR was used to assess the the expression of M2 macrophages markers. (**E**) FCM was used to measure the expression of the M2 macrophage marker (CD163) following treatment with MG-63 exosomes and HOS exosomes. (**F**) qRT-PCR and (**G**) ELISA were used to detect the expression of M2 markers (Arg-1, Ym1 and CD163) and M1 markers (CD86 and iNOS) following treatment with MG-63 exosomes and HOS exosomes. (**H**, **I**) The expression of M2 markers (Arg-1, Ym1 and CD163) and M1 markers (CD86 and iNOS) were detected after treated with MG-63 anti-miR-487a exosomes and HOS anti-miR-487a exosomes with qRT-PCR (**H**) and ELISA (**I**) (*$p<0.05$; **$p<0.01$; ***$p<0.001$)

indicated that when miR-487a was overexpressed or silenced, Notch2's mRNA and protein levels were either down- or up-regulated. Then, we isolated sEVs-miR-487a from osteosarcoma cells (MG-63 sEVs and HOS sEVs). qRT-PCR (Fig. 4D) and western blot (Fig. 4F and Figure S2) results also confirmed that exosomal-miR-487a directly targets Notch2 and promotes the expression of Notch2 at mRNA and protein levels. Additionally, all results showed that sEVs-miR-487a binds to Notch2 and increases both its mRNA and protein expression.

To gain further insights into the role of Notch2 in macrophages, we investigated the expression of M2 markers (Arg-1, Ym1, and CD163) in macrophages transfected with miR-487a mimics or miR-487a mimics along with si-Notch2. MiR-487a mimics elevated the expression of Arg-1, Ym1, and CD163, as seen by the FCM (Fig. 4F). However, the effects of miR-487a on macrophage polarizations were somewhat mitigated by silencing Notch 2 (Fig. 4F and H and Figure S3). Additionally, we found that sEVs carrying miR-487a can activate Notch2 in macrophages, as shown in Fig. 4I and J and Figure S4. The M2 macrophage marker CD163 was detected by flow cytometry, as illustrated in Fig. 4K. This finding supports the idea that sEVs-miR-487a, which targets Notch 2, induces the polarization of macrophages towards M2-like. Taken together, these data suggest that sEVs carrying miR-487a can activate the Notch 2/GATA 3 pathway, resulting in the production of IL-4. The increased levels of IL-4 further promote the polarization of macrophages towards the M2 phenotype.

sEVs-miR-487a induces M2 macrophage polarization and facilitates the EMT of osteosarcoma

The role of sEVs-miR-487a- induced M2 macrophages on the migration and invasion of osteosarcoma cells was examined using the Transwell Assay (Fig. 5A). We collected the medium from pretreated macrophages with exogenous miR-487a mimics and then employed the medium to treat MG-63 cells and U2OS cells. As shown in Fig. 5B and C, exogenous miR-487a mimics increased the cells' number of migration and invasion. Moreover, we isolated sEVs from MG-63 and U2OS cells, and macrophages were cultured with MG-63 sEVs (30 μg/mL) or HOS sEVs (30 μg/mL) for 24 h, then the condition medium was collected. Consequently, MG-63 cells and U2OS cells were incubated with the condition medium for 48 h. Migration and invasion results suggested that sEVs-miR-487a significantly promotes the development of osteosarcoma (Fig. 5D and E). To further explore whether sEVs-miR-487a activation of M2 macrophages promotes the EMT of osteosarcoma cells, we performed western blot analysis. The results (Fig. 5F and G and Figure S5-Figure S6) demonstrated that the expression level of E-cadherin protein was decreased upon treatment with sEVs carrying miR-487a. However, N-cadherin, Vimentin, and Twist showed opposite results, indicating an increase in their expression levels after treatment with sEVs-miR-487a. Additionally, the cell proliferation results (Fig. 5H and I) shown that osteosarcoma cells secreted sEVs which stimulate the proliferation of osteosarcoma cells, compared with the control group ($P<0.01$). Together, sEVs-miR-487a induces M2 macrophage polarization and facilitates the EMT of osteosarcoma cells.

sEVs-miR-487a induces the polarization of M2 macrophage to facilitate the lung metastasis of osteosarcoma cells

To further confirm the influence of sEVs-miR-487a on macrophage polarization, which regulates osteosarcoma development in vivo. MG-63 cells and conditioned macrophages (pretreated with MG-63 sEVs or PBS) were co-injected *i.v.* into BALB/c nude mice. After 7 weeks, the mice in the sEVs-treated group exhibited a higher number of lung metastatic nodules that were also larger in size compared to the control group (Fig. 6A and B). Subsequently, the weight of mice in the control group was higher than that of the mice in the MG-63 sEVs pre-treated macrophages group (Fig. 6C). The results demonstrated that sEVs-miR-487a promotes osteosarcoma lung metastasis in vivo.

MiR-487a is related to osteosarcoma lung metastasis in plasma sEVs

To determine the function of miR-487a in clinical samples, we measured its expression level in patients with lung metastases from osteosarcoma, using non-metastasis individuals as a control group. Patients with lung metastases from osteosarcoma ($n=8$) expressed more

miR-487a than patients in the control group ($n=8$) (Fig. 6D). Consequently, to investigate whether sEVs carrying miR-487a are associated with osteosarcoma lung metastasis, we isolated sEVs from the plasma of different groups. Then miR-487a was detected with qRT-PCR. The results showed that the expression level of sEVs carrying miR-487a was higher in lung metastases from osteosarcoma patients compared to other groups. It was significantly lower in patients without lung metastases from osteosarcoma, and the lowest level was observed in healthy volunteers (Fig. 6E). Surprisingly, in those patients with lung metastasis, the relative abundance of miR-487a was higher in the metastasis site than in the para-metastatic site (Fig. 6F). All these findings suggest that miR-487a is a key oncogenic miRNA that promotes osteosarcoma lung metastasis.

Discussion

Osteosarcoma is a form of aggressive bone tumor that constitutes one-fifth of all primary bone sarcomas. Osteosarcoma patients have a 5-year survival rate of only 20% due to the high risk of lung and bone metastases [28]. As a result, it is crucial to explore the factors that underlie osteosarcoma growth and metastasis, as well as to improve the therapeutic efficacy of osteosarcoma. In this study, our findings suggest that miR-487a can target Notch 2 and activate GATA 3-induced IL-4 secretion. The increased production of IL-4, in turn, promotes the polarization of M2-type tumor-associated macrophages (TAMs) and contributes to the promotion of lung metastasis in osteosarcoma.

TAMs are a subclass of immune cells that secrete cytokines to control the initiation and growth of tumor cells in the surrounding tissue [29]. Macrophages, which can exist as both alternatively activated M2 macrophages and classically activated M1 macrophages, are naturally malleable. The development and metastasis of tumours are accelerated by anti-inflammatory substances released by M2-type macrophages, which were involved in the poor prognosis of osteosarcoma [8]. Recently, the crucial role of sEVs in regulating the polarization of macrophage into M1/M2 types has been reported [30, 31]. In the current study, macrophages isolated from human blood were co-cultured with sEVs derived from osteosarcoma cells highly expressing miR-487a. As a result of this co-culture, the macrophages demonstrated M2-like characteristics. In TME, M2-polarised macrophages accelerate tumor EMT, growth, and metastasis [32]. Our results show that osteosarcoma cell-derived sEVs-miR-487a could facilitate the polarization of macrophages toward M2 type, as evidenced by up-regulation of M2 markers (CD206, Arg-1, and IL-10), and do not influence the expression of M1 markers (iNOS and CD86).

Increased infiltration of M2 tumor-associated macrophages (M2-TAMs) has been associated with osteosarcoma metastasis. Epithelial-mesenchymal transition (EMT) is recognized as a key process in tumor metastasis, including in the context of osteosarcoma [33], plays a vital role in osteosarcoma metastasis. It is necessary to deeply explore the underlying mechanisms of EMT, macrophage polarization, and the diagnosis of osteosarcoma. We demonstrated a new anti-tumor mechanism by which sEVs induce macrophages toward M2-type, thereby promoting EMT, migration, and invasion of tumor cells. It was discovered that tumor cells secrete sEVs that can affect the function of their target cells by activating a specific signaling pathways [34]. Additionally, our study reported that sEVs carrying miR-487a could enhance the progression of osteosarcoma by affecting the interaction between TAMs and osteosarcoma cells. Furthermore, compared to individuals with lung metastases from osteosarcoma, those without lung metastases had considerably lower plasma levels of sEVs-miR-487a. This suggests that plasma sEVs-miR-487a may have clinical significance in predicting osteosarcoma lung metastases.

We identified the signaling pathway involved in macrophage polarization to confirm the mechanism of sEVs-miR-487a boosting tumor cell polarization. Notably, our data show that sEVs-miR-487a can target Notch2 and regulate GATA3 to modulate the activity of the Notch2/GATA3/IL-4 axis in macrophage. The polarization of macrophages was facilitated by GATA3-induced IL-4 production, which required the activation of the Notch pathway [35]. Generally, IL-4 can trigger M2 polarization of macrophages [36]. Moreover, GATA3 is a transcription factor that participate in the polarization of M2 macrophages [37], and shRNA knockout of GATA3 can suppress the polarization of M2 macrophages [38]. Targeting Notch2 and controlling GATA3-induced IL-4 secretion [35], as well as preventing CD4+T cells from suppressing the production of IL-4 [14], have been shown to influence the polarization of macrophages. Th2 cells, which respond to the release of IL-4, IL-15, and IL-13, rely on the presence of GATA3 for their development [39]. STAT6 is activated and phosphorylated by IL-4, which allowed STAT6 to induce the M2 type of macrophage [40]. STAT6 can be activated by IL-4 as a transcriptional repressor in macrophages [40].

sEVs, also known as extracellular vesicles, are membranous structures produced by various cells. These vesicles play a crucial role in facilitating cell-to-cell communication between immune cells and cancer cells within the tumor microenvironment (TME). miRNAs

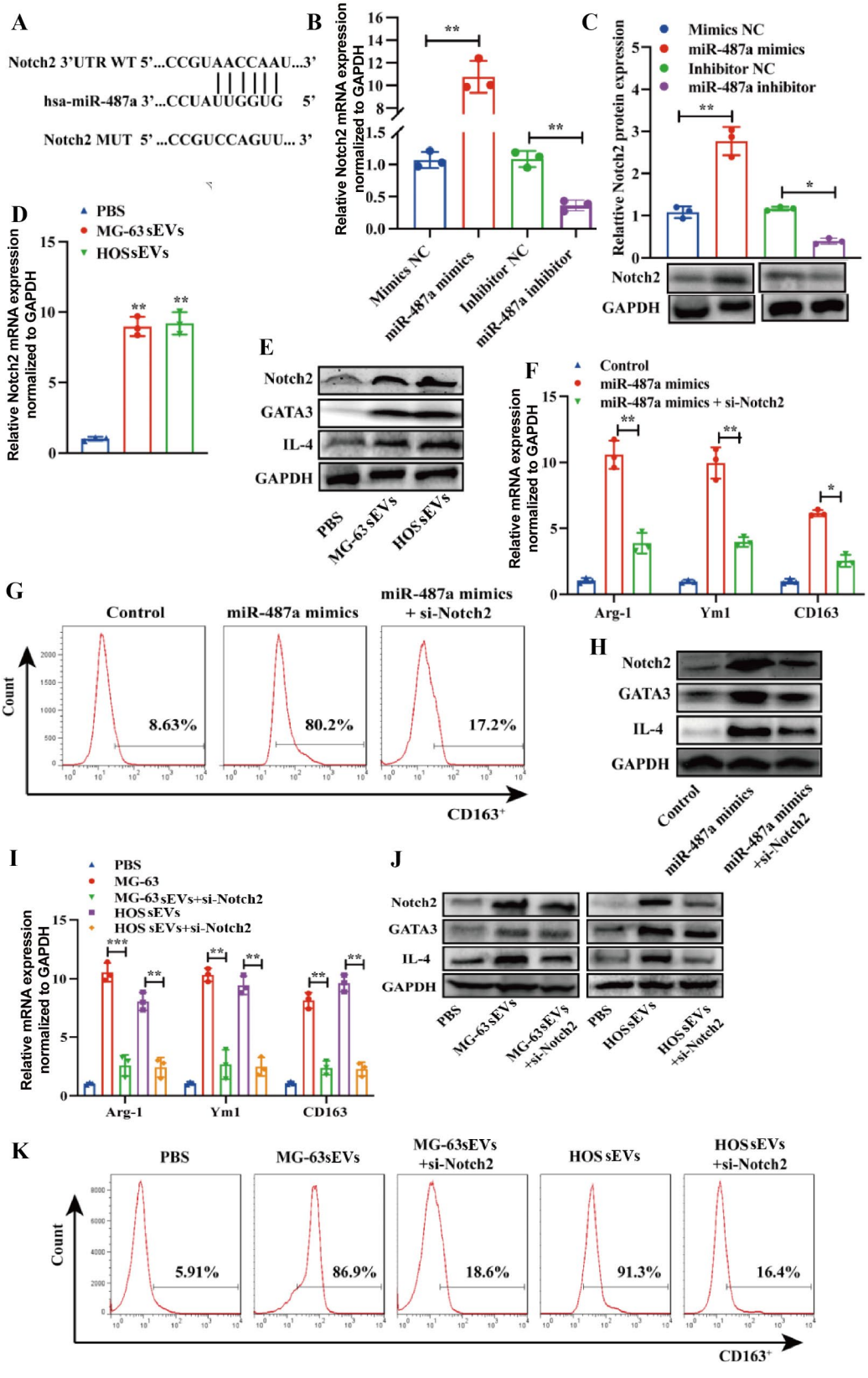

Fig. 4 (See legend on next page.)

(See figure on previous page.)

Fig. 4 Exosomal-miR-487a targets Notch2 and induces M2 polarization by activating GATA3. (**A**) TargetScan is used for miR-487a target gene prediction. (**B**) Macrophages' relative Notch2 mRNA expression. (**C**) Western blot was used to confirm the expression of Notch2 in macrophages was discovered following treatment with miR-487a mimics or inhibitor. (**D**) Expression of Notch2 in macrophages after treatment with MG-63 exosomes and HOS exosomes. (**E**) Expression of Notch2, GATA3, and IL-4 proteins in macrophages following treatment with MG-63 exosomes and HOS exosomes. (**F-G**) Macrophages were transfected either with miR-487a plus si-Notch2 or miR-487a mimics. The expression of M2 markers (Arg-1, Ym1, and CD163) was assessed using qRT-PCR (**F**) and FCM (**G**). (**H**) Western blot analysis was used to identify components of the Notch2/GATA3 pathway. (**I**, **J**) MG-63 exosomes, MG-63 exosomes plus si-Notch2, HOS exosomes, or HOS exosomes plus si-Notch2 were applied to macrophages. (**K**) FCM was used to confirm the expression of CD163, an M2 marker (*$p<0.05$; **$p<0.01$; ***$p<0.001$)

carried by sEVs are indeed delivered to target cells, where they have the ability to influence and modulate the progression of these cells. Previous studies have reported that tumor cells secrete sEVs-miRNA which could facilitate the polarization of macrophages toward the M2 type [21]. It has been shown that sEVs-miR-221, produced from mammary epithelial cells, encourages macrophage polarization toward M1-type [41]. On the other hand, sEVs-miR-29a-3p, secreted by oral squamous cell carcinoma, mediates the polarization of M2-type macrophages [42]. Furthermore, exosomal miR-92a-3p, derived from high-metastatic cancer cells, has been shown to promote the metastasis and epithelial-mesenchymal transition (EMT) of low-metastatic cancer cells [43].

Furthermore, sEVs can be collected directly from patients' bodily fluids, and sEVs miRNA may serve as a non-invasive biomarker to monitor a patient's illness development. According to our research, patients with lung metastases from osteosarcoma exhibited the highest level of miR-487a expression. In contrast, patients without lung metastases had the lowest level of miR-487a expression, comparable to that observed in the group of healthy volunteers. These findings indicate a significant correlation between lung metastasis in osteosarcoma and high expression of sEVs carrying miR-487a. This suggests that miR-487a in plasma-derived sEVs has the potential to serve as a predictive biomarker for the diagnosis of osteosarcoma.

Conclusion

In summary, our results demonstrate that miR-487a, derived from osteosarcoma cells, can be delivered to macrophages through sEVs. Subsequently, it promotes the polarization of macrophages towards an M2-like phenotype by targeting Notch2 and activating the GATA3 pathway. The activation of macrophages promotes epithelial-mesenchymal transition (EMT), subsequently enhances the migration, invasion, and lung metastasis of osteosarcoma cells. In particular, our data reveal a novel mechanism in which osteosarcoma cell-derived sEVs carrying miR-487a play a role in the development of osteosarcoma by modulating the polarization of macrophages towards an M2 phenotype within the tumor microenvironment (TME).

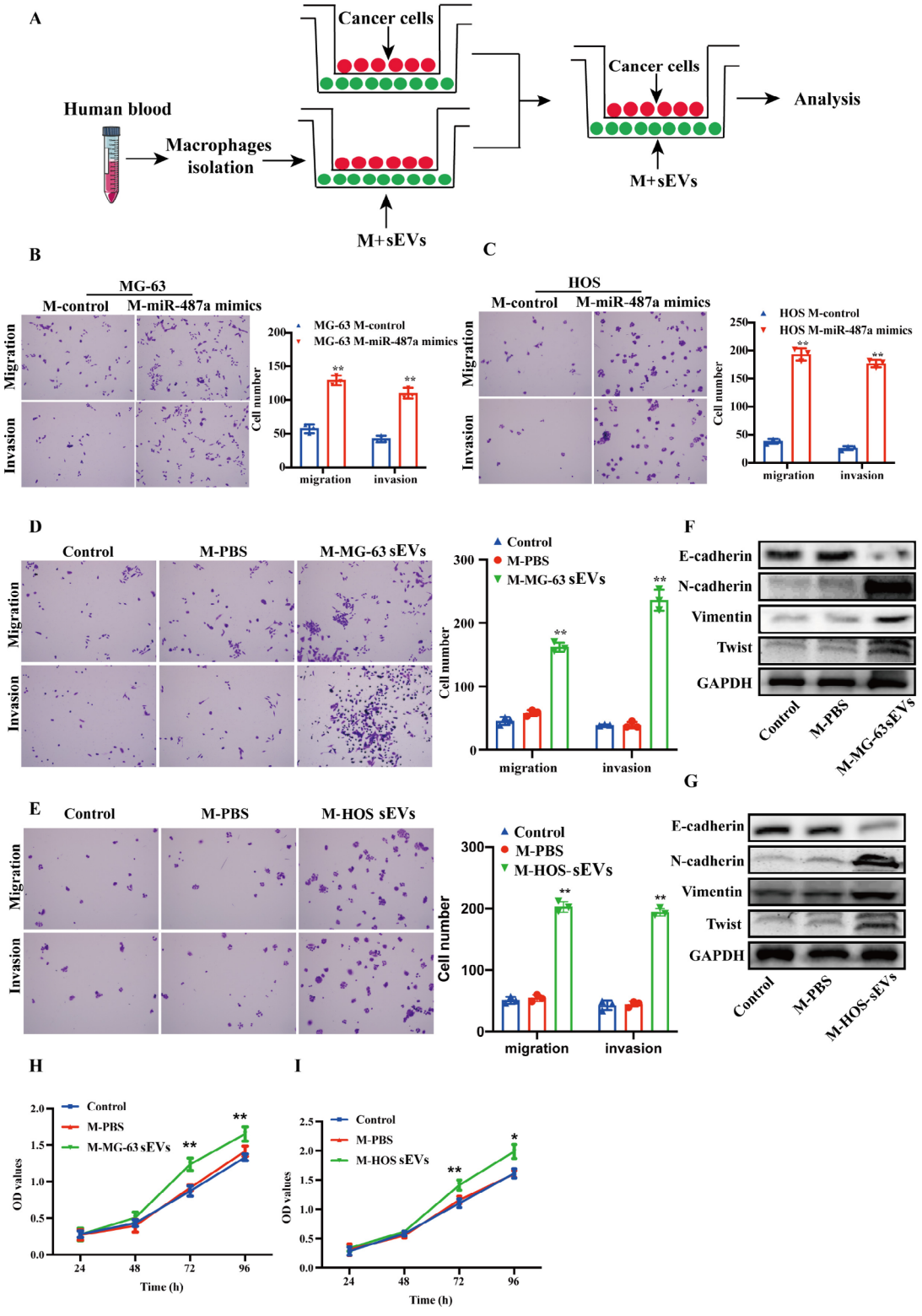

Fig. 5 Exosomal-miR-487a polarizes M2 macrophages to encourage the migration and invasion of osteosarcoma cells. (**A**) Diagrammatic representation of the in vitro indirect coculture system. (**B-C**) After MG-63/HOS cells were fed with macrophage media and transfected with miR-487a mimics, the transwell assay was used to assess cell migration and invasion. (**D-G**) Macrophages were treated with MG-63 exosomes and HOS exosomes (30 μg/mL), and then the conditioned medium was collected to co-culture with MG-63 and HOS cells. Migration and invasion were assessed using the transwell assay (**D**, **E**) and western blot analysis was used to determine the expression of invasion-related proteins (**F**, **G**). (**H-I**) The cell proliferation was performed with CCK-8 assay (*p<0.05; **p<0.01; ***p<0.001)

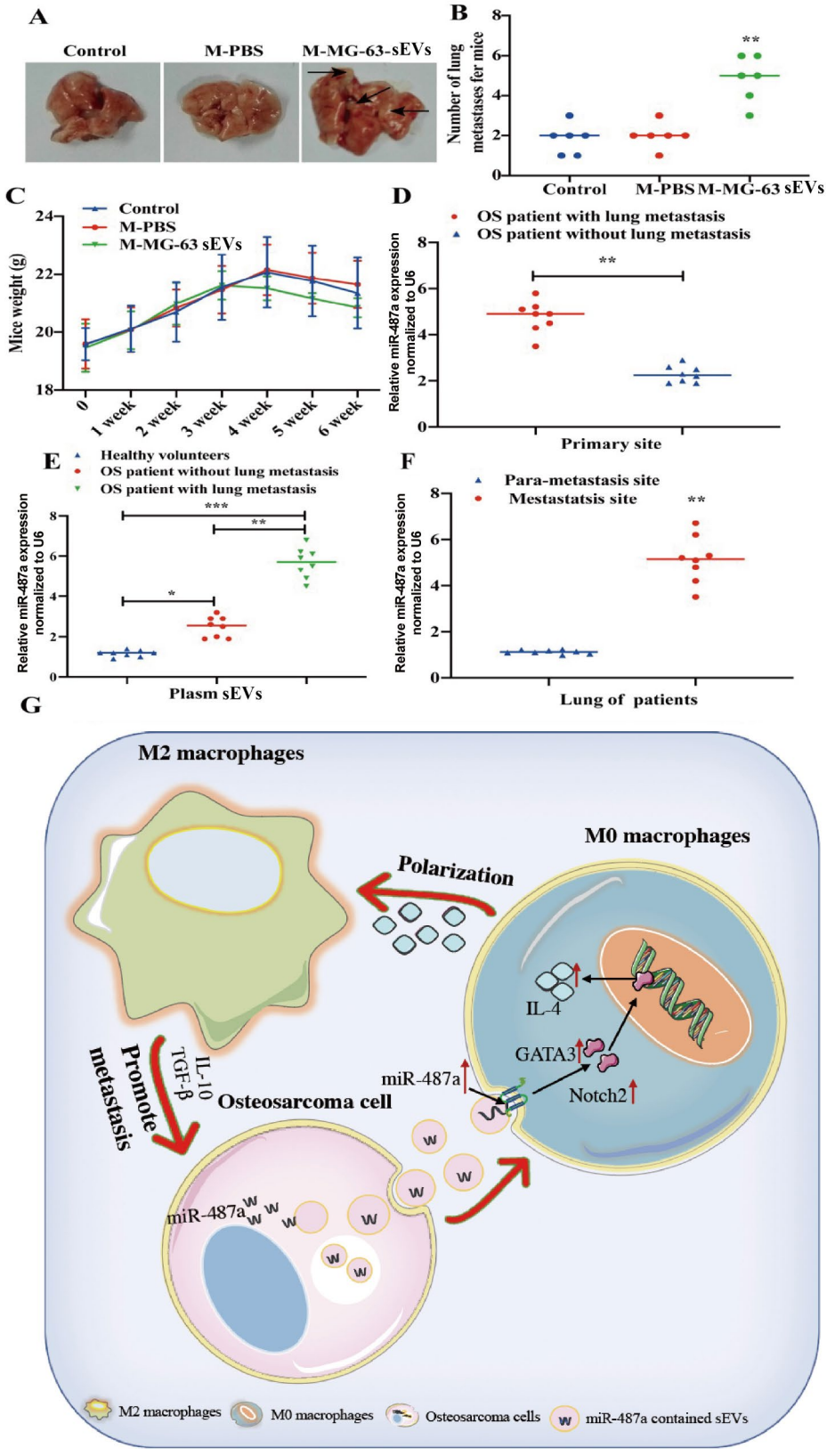

Fig. 6 (See legend on next page.)

(See figure on previous page.)

Fig. 6 Exosomal-miR-487a induces M2 macrophage polarization, which promotes osteosarcoma cell metastasis. (**A**) Representative images of lung metastasis in nude mice resulting from MG-63 cells injected alone or co-injected with macrophages pretreated with MG-63 exosomes. (**B**) The number of metastatic nodules in each group. (**C**) The weight of mice in each group. (**D**) The expression of miR-487a in osteosarcoma patients with lung metastasis and in osteosarcoma primary tissues with or without lung metastasis ($n=8$ for each group). (**E**) The level of plasma exosomal-miR-487a in healthy volunteers, osteosarcoma primary tissues with or without lung metastasis ($n=8$ for each group). (**F**) The level of miR-487a in osteosarcoma patients with lung metastasis was measured using qRT-PCR (para-metastasis site vs. metastasis, $n=8$ for each group). (**G**) The graphic abstract of this sduty (*$p<0.05$; **$p<0.01$; ***$p<0.001$)

Supplementary Information

The online version contains supplementary material available at https://doi.org/10.1186/s12935-024-03488-x.

Supplementary Material 1

Author contributions

P.P. W. was drafted original manuscript. L. Y. helped us revised the grammar and sentence structure of this manuscript.W.J. L., F.X., Y.L., and J. D. handled the statistical analysis. W.Y. L. is responsible for reviewing and editing.

Funding

The National Natural Science Foundation of China (Grant No. 82203104), the Shanghai Municipal Health Commission Fund (Grant No. PWRI2021-11), and the Shanghai Pudong New District Health Committee's Key Disciplines of Clinical Pharmacy (PWZxk2022-26) all provided funding for this study.

Data availability

No datasets were generated or analysed during the current study.

Declarations

Conflict of interest

The author has no conflicts about article preparation.

Consent fto publications

The author has reviewed and agreed the manuscript for publication.

Ethics permission and agreement to participate

The human and animal experiment were authorized via the Taizhou People's Hospital of Nanjing Medical University.

Received: 19 March 2024 / Accepted: 19 August 2024
Published online: 31 August 2024

References

1. Trujillo-Paolillo A, Tesser-Gamba F, Seixas Alves MT, Filho RJG, Oliveira R, Petrilli AS, Toledo SRC. Pharmacogenetics of the primary and metastatic osteosarcoma: gene expression Profile Associated with Outcome. Int J Mol Sci 2023, 24(6).
2. Nirala BK, Yamamichi T, Petrescu DI, Shafin TN, Yustein JT. Decoding the impact of Tumor Microenvironment in Osteosarcoma Progression and Metastasis. Cancers (Basel) 2023, 15(20).
3. Liao Z, Lim JJH, Lee JXT, Chua D, Vos MIG, Yip YS, Too CB, Cao H, Wang JK, Shou Y et al. Attenuating epithelial-to-mesenchymal transition in Cancer through Angiopoietin-Like 4 inhibition in a 3D Tumor Microenvironment Model. Adv Healthc Mater 2023:e2303481.
4. Zhao Y, Shen M, Wu L, Yang H, Yao Y, Yang Q, Du J, Liu L, Li Y, Bai Y. Stromal cells in the tumor microenvironment: accomplices of tumor progression? Cell Death Dis. 2023;14(9):587.
5. Christofides A, Strauss L, Yeo A, Cao C, Charest A, Boussiotis VA. The complex role of tumor-infiltrating macrophages. Nat Immunol. 2022;23(8):1148–56.
6. Heymann MF, Lezot F, Heymann D. The contribution of immune infiltrates and the local microenvironment in the pathogenesis of osteosarcoma. Cell Immunol. 2019;343:103711.
7. Xiao Q, Zhang X, Wu Y, Yang Y. Inhibition of macrophage polarization prohibits growth of human osteosarcoma. Tumour Biol. 2014;35(8):7611–6.
8. Liu J, Geng X, Hou J, Wu G. New insights into M1/M2 macrophages: key modulators in cancer progression. Cancer Cell Int. 2021;21(1):389.
9. Biswas SK, Mantovani A. Macrophage plasticity and interaction with lymphocyte subsets: cancer as a paradigm. Nat Immunol. 2010;11(10):889–96.
10. Chen W, Jiang J, Xia W, Huang J. Tumor-related exosomes contribute to tumor-promoting Microenvironment: an immunological perspective. J Immunol Res. 2017;2017:1073947.
11. Misiorek JO, Przybyszewska-Podstawka A, Kalafut J, Paziewska B, Rolle K, Rivero-Muller A, Nees M. Context matters: NOTCH signatures and Pathway in Cancer Progression and Metastasis. Cells 2021, 10(1).
12. Colombo M, Mirandola L, Chiriva-Internati M, Basile A, Locati M, Lesma E, Chiaramonte R, Platonova N. Cancer cells exploit Notch Signaling to redefine a supportive cytokine milieu. Front Immunol. 2018;9:1823.
13. Maraver A, Fernandez-Marcos PJ, Cash TP, Mendez-Pertuz M, Duenas M, Maietta P, Martinelli P, Munoz-Martin M, Martinez-Fernandez M, Canamero M, et al. NOTCH pathway inactivation promotes bladder cancer progression. J Clin Invest. 2015;125(2):824–30.
14. Fang TC, Yashiro-Ohtani Y, Del Bianco C, Knoblock DM, Blacklow SC, Pear WS. Notch directly regulates Gata3 expression during T helper 2 cell differentiation. Immunity. 2007;27(1):100–10.
15. Tanaka S, Tsukada J, Suzuki W, Hayashi K, Tanigaki K, Tsuji M, Inoue H, Honjo T, Kubo M. The interleukin-4 enhancer CNS-2 is regulated by notch signals and controls initial expression in NKT cells and memory-type CD4 T cells. Immunity. 2006;24(6):689–701.
16. Tanaka S, Motomura Y, Suzuki Y, Yagi R, Inoue H, Miyatake S, Kubo M. The enhancer HS2 critically regulates GATA-3-mediated Il4 transcription in T(H)2 cells. Nat Immunol. 2011;12(1):77–85.
17. Wei W, Li ZP, Bian ZX, Han QB. Astragalus Polysaccharide RAP induces macrophage phenotype polarization to M1 via the Notch Signaling Pathway. Molecules 2019, 24(10).
18. Huang G, Lin G, Zhu Y, Duan W, Jin D. Emerging technologies for profiling extracellular vesicle heterogeneity. Lab Chip. 2020;20(14):2423–37.
19. Zhou X, Jia Y, Mao C, Liu S. Small extracellular vesicles: non-negligible vesicles in tumor progression, diagnosis, and therapy. Cancer Lett. 2024;580:216481.
20. Yang X, Wang M, Lin B, Yao D, Li J, Tang X, Li S, Liu Y, Xie R, Yu S. miR-487a promotes progression of gastric cancer by targeting TIA1. Biochimie. 2018;154:119–26.
21. Zhao S, Mi Y, Guan B, Zheng B, Wei P, Gu Y, Zhang Z, Cai S, Xu Y, Li X, et al. Tumor-derived exosomal miR-934 induces macrophage M2 polarization to promote liver metastasis of colorectal cancer. J Hematol Oncol. 2020;13(1):156.
22. Ma M, He M, Jiang Q, Yan Y, Guan S, Zhang J, Yu Z, Chen Q, Sun M, Yao W, et al. MiR-487a promotes TGF-beta1-induced EMT, the Migration and Invasion of breast Cancer cells by directly targeting MAGI2. Int J Biol Sci. 2016;12(4):397–408.
23. Chang RM, Xiao S, Lei X, Yang H, Fang F, Yang LY. miRNA-487a promotes proliferation and metastasis in Hepatocellular Carcinoma. Clin Cancer Res. 2017;23(10):2593–604.
24. Merah-Mourah F, Cohen SO, Charron D, Mooney N, Haziot A. Identification of Novel Human Monocyte subsets and evidence for phenotypic groups defined by interindividual variations of expression of Adhesion molecules. Sci Rep. 2020;10(1):4397.
25. Chen C, Tan R, Wong L, Fekete R, Halsey J. Quantitation of microRNAs by real-time RT-qPCR. Methods Mol Biol. 2011;687:113–34.
26. Wang P, Wang H, Huang Q, Peng C, Yao L, Chen H, Qiu Z, Wu Y, Wang L, Chen W. Exosomes from M1-Polarized macrophages enhance Paclitaxel Antitumor activity by activating macrophages-mediated inflammation. Theranostics. 2019;9(6):1714–27.
27. Jiang C, Fang X, Zhang H, Wang X, Li M, Jiang W, Tian F, Zhu L, Bian Z. AMD3100 combined with triptolide inhibit proliferation, invasion and metastasis and induce apoptosis of human U2OS osteosarcoma cells. Biomed Pharmacother. 2017;86:677–85.

28. Wang X, Qin G, Liang X, Wang W, Wang Z, Liao D, Zhong L, Zhang R, Zeng YX, Wu Y, et al. Targeting the CK1alpha/CBX4 axis for metastasis in osteosarcoma. Nat Commun. 2020;11(1):1141.
29. Yang Q, Guo N, Zhou Y, Chen J, Wei Q, Han M. The role of tumor-associated macrophages (TAMs) in tumor progression and relevant advance in targeted therapy. Acta Pharm Sin B. 2020;10(11):2156–70.
30. Moradi-Chaleshtori M, Bandehpour M, Heidari N, Mohammadi-Yeganeh S, Mahmoud Hashemi S. Exosome-mediated miR-33 transfer induces M1 polarization in mouse macrophages and exerts antitumor effect in 4T1 breast cancer cell line. Int Immunopharmacol. 2021;90:107198.
31. Wang D, Wang X, Si M, Yang J, Sun S, Wu H, Cui S, Qu X, Yu X. Exosome-encapsulated miRNAs contribute to CXCL12/CXCR4-induced liver metastasis of colorectal cancer by enhancing M2 polarization of macrophages. Cancer Lett. 2020;474:36–52.
32. Fan QM, Jing YY, Yu GF, Kou XR, Ye F, Gao L, Li R, Zhao QD, Yang Y, Lu ZH, et al. Tumor-associated macrophages promote cancer stem cell-like properties via transforming growth factor-beta1-induced epithelial-mesenchymal transition in hepatocellular carcinoma. Cancer Lett. 2014;352(2):160–8.
33. Cersosimo F, Lonardi S, Bernardini G, Telfer B, Mandelli GE, Santucci A, Vermi W, Giurisato E. Tumor-Associated macrophages in Osteosarcoma: from mechanisms to Therapy. Int J Mol Sci 2020, 21(15).
34. Xiang X, Liu Y, Zhuang X, Zhang S, Michalek S, Taylor DD, Grizzle W, Zhang HG. TLR2-mediated expansion of MDSCs is dependent on the source of tumor exosomes. Am J Pathol. 2010;177(4):1606–10.
35. Lin X, Wang S, Sun M, Zhang C, Wei C, Yang C, Dou R, Liu Q, Xiong B. Correction to: miR-195-5p/NOTCH2-mediated EMT modulates IL-4 secretion in colorectal cancer to affect M2-like TAM polarization. J Hematol Oncol. 2019;12(1):122.
36. Witherel CE, Sao K, Brisson BK, Han B, Volk SW, Petrie RJ, Han L, Spiller KL. Regulation of extracellular matrix assembly and structure by hybrid M1/M2 macrophages. Biomaterials. 2021;269:120667.
37. Zhong Y, Yi C. MicroRNA-720 suppresses M2 macrophage polarization by targeting GATA3. Biosci Rep 2016, 36(4).
38. El-Arabey AA, Denizli M, Kanlikilicer P, Bayraktar R, Ivan C, Rashed M, Kabil N, Ozpolat B, Calin GA, Salama SA, et al. GATA3 as a master regulator for interactions of tumor-associated macrophages with high-grade serous ovarian carcinoma. Cell Signal. 2020;68:109539.
39. Tindemans I, Serafini N, Di Santo JP, Hendriks RW. GATA-3 function in innate and adaptive immunity. Immunity. 2014;41(2):191–206.
40. Czimmerer Z, Daniel B, Horvath A, Ruckerl D, Nagy G, Kiss M, Peloquin M, Budai MM, Cuaranta-Monroy I, Simandi Z, et al. The transcription factor STAT6 mediates direct repression of inflammatory enhancers and limits activation of alternatively polarized macrophages. Immunity. 2018;48(1):75–e9076.
41. Cai J, Qiao B, Gao N, Lin N, He W. Oral squamous cell carcinoma-derived exosomes promote M2 subtype macrophage polarization mediated by exosome-enclosed miR-29a-3p. Am J Physiol Cell Physiol. 2019;316(5):C731–40.
42. Cai M, Shi Y, Zheng T, Hu S, Du K, Ren A, Jia X, Chen S, Wang J, Lai S. Mammary epithelial cell derived exosomal MiR-221 mediates M1 macrophage polarization via SOCS1/STATs to promote inflammatory response. Int Immunopharmacol. 2020;83:106493.
43. Yang B, Feng X, Liu H, Tong R, Wu J, Li C, Yu H, Chen Y, Cheng Q, Chen J, et al. High-metastatic cancer cells derived exosomal miR92a-3p promotes epithelial-mesenchymal transition and metastasis of low-metastatic cancer cells by regulating PTEN/Akt pathway in hepatocellular carcinoma. Oncogene. 2020;39(42):6529–43.

Publisher's note